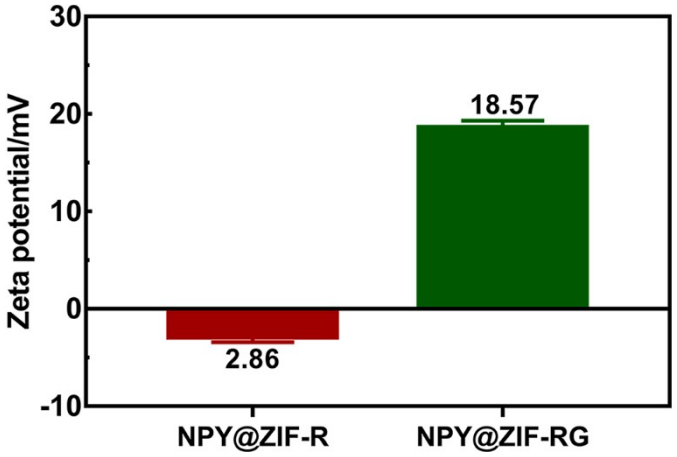


**Fig. S1. Zeta potentials of nanoparticles.**

Zeta potentials of NPY@ZIF-R (red) and NPY@ZIF-RG (green).

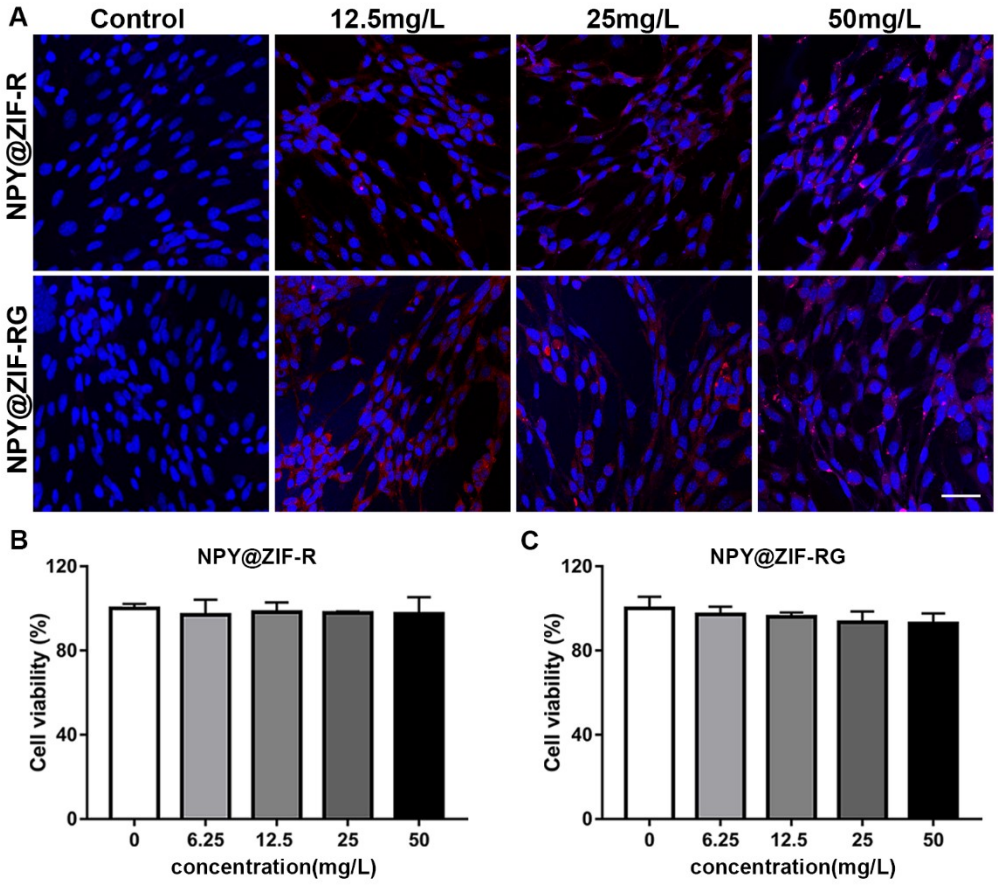


**Fig. S2. Fluorescence imaging and viability of NPY@ZIF-R and NPY@ ZIF-RG.**

(A) Fluorescence images of HT22 cells following NPY@ZIF-R and NPY@ZIF-RG incubation for 24 h at different concentrations (0,12.5, 25 and 50 mg/L). (B-C) The cell viabilities of NPY@ZIF-R and NPY@ZIF-RG at different concentrations from 6.25 to 50 mg/L (ANOVA, $P>0.05$). Scale bars: 50 μm.

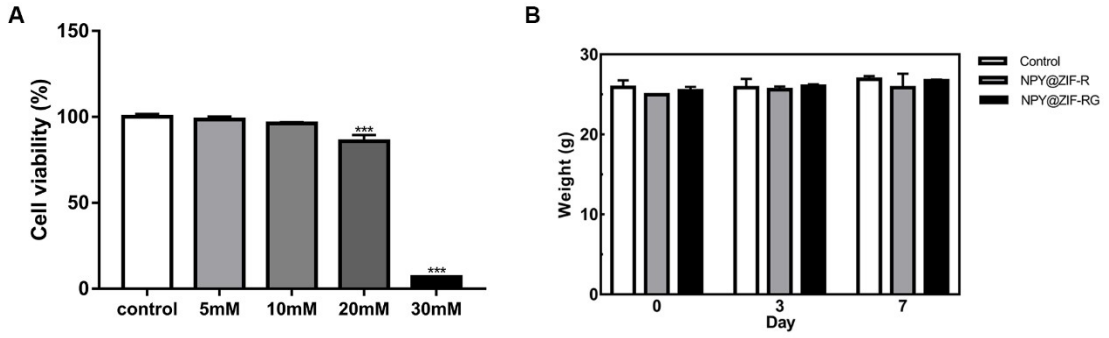


**Fig. S3. Cytotoxicity of Glu and the body weight of mice.**

(A) The cell viabilities of Glu on HT22 cells from different concentrations (0, 5, 10, 20 and 30 mM) (ANOVA; ***$P<0.001$). (B) The body weight of mice following NPY@ZIF-R and NPY@ZIF-RG treatment at 0, 3, 7 days, respectively (ANOVA; $P>0.05$).

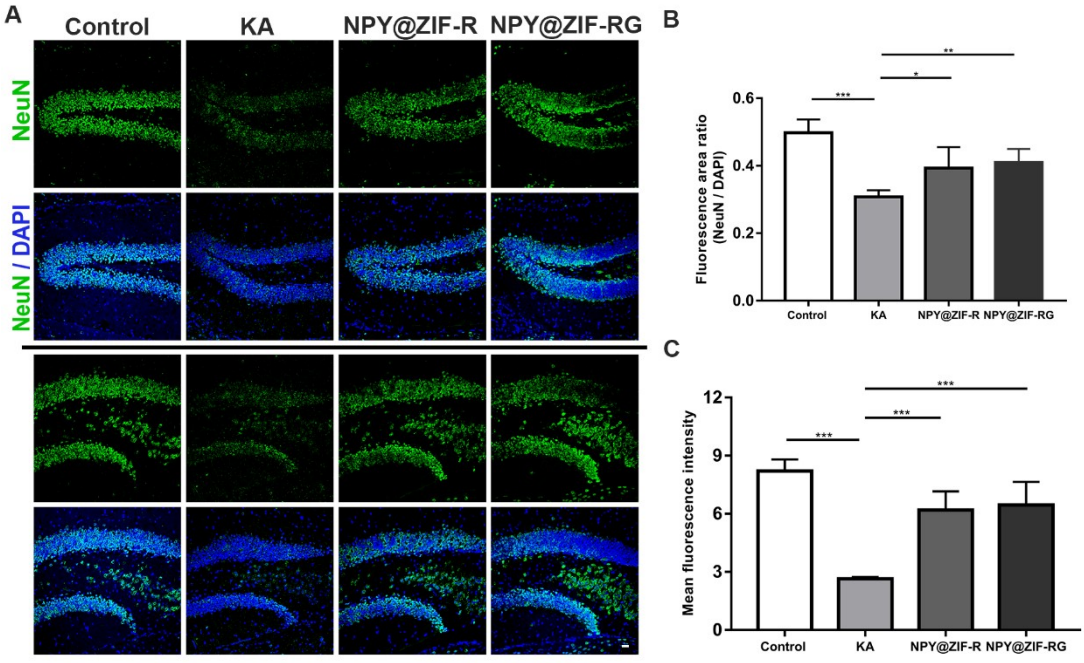

**Fig. S4. Neuronal damage and recovery in KA-induced seizure.**

(A) Representive images of NeuN immunostaining from hippocampal regions in the control, KA, NPY@ZIF-R and NPY@ZIF-RG groups. (B and C) Quantification of the ratio of NeuN/DAPI fluorescence area and the mean fluorescence intensity of NeuN-positive cells (ANOVA; **P*<0.05, ***P*<0.01, ****P*<0.001). Scale bars: 10 μm.